Stroboscopic torsion pendulum

M. Bassan[a,b,*], L.Di Fiore[c], A. Grado[d,c], Y. Minenkov[b], E.Reali[a,b], G.Pucacco[a,b]

[a] *Dipartimento di Fisica, Università di Roma "Tor Vergata", I-00133 Roma, Italy*
[b] *Istituto Nazionale di Fisica Nucleare - Sezione Roma2, I-00133 Roma, Italy*
[c] *Istituto Nazionale di Fisica Nucleare - Sezione di Napoli, I-80126, Napoli, Italy*
[d] *Istituto Nazionale di Astrofisica - Osservatorio Astronomico di Capodimonte, I-80126 Napoli, Italy*

Abstract

We report on a simple, inexpensive readout for torsion pendulums, suitable for robust applications like teaching-lab equipment or monitoring of large amplitude oscillations. A short light pulse is recorded every time a reflective band on the pendulum inertial member passes in front of the sensor, an infrared LED pair (emitter-receiver). Simple algebraic manipulations on the time series of these pulses arrival times allow to extract the resonant frequency as well as the decay time of the pendulum. This readout is insensitive to the amplitude of oscillation and is therefore suitable for monitoring torsional oscillations of large amplitude, where traditonal readouts like optical levers or autocollimators encounter dynamic range limitations.

Keywords: Torsion Pendulum, Optical Readout, Stroboscopic

1. Introduction and Motivation

The torsion pendulum is still, after over two centuries from its conception, a widely used instrument to measure and characterize weak forces or torques [1, 2, 3]. The dynamics of a torsion pendulum, like any second-order system, is described by just three parameters: the moment of inertia of its inertial member I_0, the torsion constant of the suspending fiber κ, and the dissipation time constant τ (or the quality factor Q); these parameters need to be evaluated with a precision that directly feeds into the error budget of the experiment. The torsion constant is usually derived by measuring the pendulum resonant frequency, or oscillation period T, via the basic relation $(2\pi/T)^2 = \kappa/I_0$. However, there are instances, in some sophisticated devices, where this is not so straightforward, and the torsion constant of the fibers must be characterized on a separate test bench: this happens when the inertial mass has a complex shape or, relevant to our research, in the case of a double pendulum.

*Correspondig author: bassan@roma2.infn.it

In a double pendulum, like the PETER [4, 5] apparatus, designed to simultaneously measure one component of both force and torque acting on its inertial member (often referred to as Test Mass), two torsion fibers are deployed in cascade, producing two coupled torsional modes: in this case, disentangling the coupled resonant frequencies to derive the fiber constants is not a simple task, as inversion of the eigenfrequency equation is not unique. We were therefore forced to separately measure the torsional constant of each fiber (in our case, 100 and 25 μm in diameter), in order to obtain a full characterization of the apparatus. Therefore, we developed a simple apparatus, to the purpose of characterizing Tungsten fibers, that were then deployed in the composite, double torsion pendulum PETER. In this paper we describe such apparatus that, despite its extreme simplicity, has some interesting features worth reporting.

The instrument described here can measure resonant frequency and decay time of torsion pendulums with simple geometries and well characterized moments of inertia. Then, as taught in freshman physics labs, the torsion constant can be derived, with an uncertitude of few parts per thousand, by linear fitting of the T^{-2} vs I_0 data. Conversely, the decay time of pendulums with same inertial member and fibers was used to evaluate different types of fasteners for the fiber. In this paper, we briefly describe the simple experimental apparatus. We then show how to extract, from the series of time stamps, both the oscillation period and the decay time. We discuss the pros and cons of performing the measurements with either two sensors or a single sensor. Some additional features, like the monitoring of the fiber unwinding, are also discussed before the conclusions.

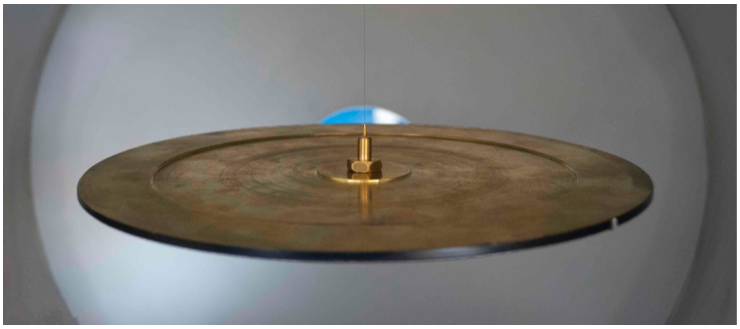

Figure 1: The largest (200 mm diameter) and heaviest (0.843 kg) inertial member, suspended to a 100 μm W wire inside the vacuum chamber. The hairline is visible on the right of the disc edge.

2. Apparatus

The pendulum is hosted in a vacuum chamber, whose main experimental space has cylindrical shape, with horizontal axis, and a a useful vertical clearance of roughly 40 cm. A horizontal opening carries a clear, see-through window.

On the top flange an O-ring sealed rotary feedthrough (quick-connector) supports a rod where the top end of the fiber is suspended (the so-called ϕ-*top*). The quick-connector allows rough rotation, from outside the vacuum, of the fiber suspension point, thus actuating oscillations around the z (vertical) axis, the ϕ degree of freedom. The opposite end of the fiber is connected to the center of an inertial member of simple shape: typically a right cylinder, threaded M4 on its center. Sizes and materials of the pendulum loads vary depending on the thickness of the fiber under test: the safe load varies from about 0.12 kg for the thinnest (25 μm) fiber we tested, to over 1.5 kg for the thickest (100 μm). We used Brass, Aluminum, Delrin, in cylinders and discs with diameters varying from 15 to 250 mm.
The lateral surface of the cylindrical load is spray-painted black, and a thin (1 mm wide) strip of alluminized mylar, the *hairline marker* is added along a generatrix. The paint adds 0.1-0.3 g depending on the area of the lateral surface of the test-mass: in the worst case, it accounts for less than 0.2% of the total mass, and modifies by less than a percent the moment of inertia. The hairline marker has an estimated mass of less than 0.05 g, and the asymmetry introduced to the cylindrical mass distribution (it is stuck to one side) is well below those given by machining tolerances.
Accounting for all measuring and machining errors, material inhomogeneity and the contribution of paint, the moment of inertia of these loads were computed with an uncertainty always smaller than 2 % and, for the larger loads, approaching 0.1 %. It is certainly possible to improve the accuracy with selected materials and more accurate measuring tools.

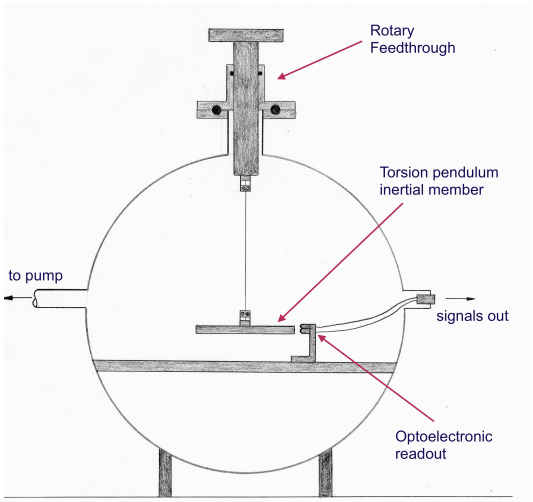

Figure 2: Schematic diagram of the apparatus, within the vacuum chamber.

We have used and compared different methods of fastening the fiber at its ends: beside the traditional gluing and clamping to brass hollow pins (similar

to those used in wire chambers), we successfully tested a new method based on a small Al vise-like block: the fiber is threaded into a soft Cu tube (0.2 mm inner diameter) and positioned between two jaws of the block (see fig.2): two M3 screws fasten together the two parts, squeezing the soft tube and blocking the fiber.

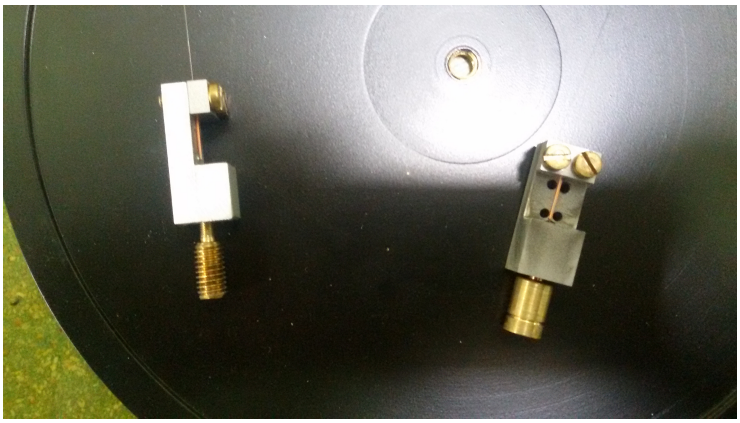

Figure 3: Squeezing blocks used to terminate the W fibers

The readout is composed by a a pair of infrared diodes (a LED emitter+ a Photodiode as receiver) contained in a single package[6] where they are positioned 3.9 mm apart. Two such packages are assembled at short horizontal distance (4 mm) on a board. Three wires plus ground are sufficient to bias two LEDs and extract the signals of the respective receivers, as shown in fig.(3). The LED board is positioned some 15 - 20 mm from the pendulum edge, at the same vertical height and with azimuthal position roughly at the center of the torsional oscillation. The pendulum is set in motion via the ϕ-*top* and when the allumined strip passes in front of the LEDs, a peak of reflected light is collected by the receiver, providing a time series of "stroboscopic" measurements (two per period) of the oscillation.
Due to its simplicity, and to the absence of dissipating components, this circuit works well, even for weeks, in our vacuum enviroment of about 0.5 mPa. This is a clear advantage over more sophisticated, linear readouts, like optical levers [7] or commercial autocollimators [8], that usually require optical ports or fiber coupling to an external source. The outputs of both sensors are then digitized by an Arduino card, sampling at frequencies up to 50 Hz: these rates are largely sufficient as we aim to measure resonant frequencies of the order of few mHz. The time series, and their time base are transferred via UBS to a PC and stored. Although we chose to trigger DAQ via an external signal generator, we have verified the internal clock of the Arduino card to disagree with the higher quality external clock by no more than 500 ppm. Measurements were taken with chamber pressure $p < 10^{-3} Pa$; we found out, however, that

residual air still exerted a marginal effect on dissipation processes, expecially on pendulums with large diameter loads.
The whole apparatus (excluding PC, vacuum gear and signal generator) is thus assembled with a cost of about 30 €, making it also suitable for teaching labs, where torsion pendulums are always popular, and can be operated in air.

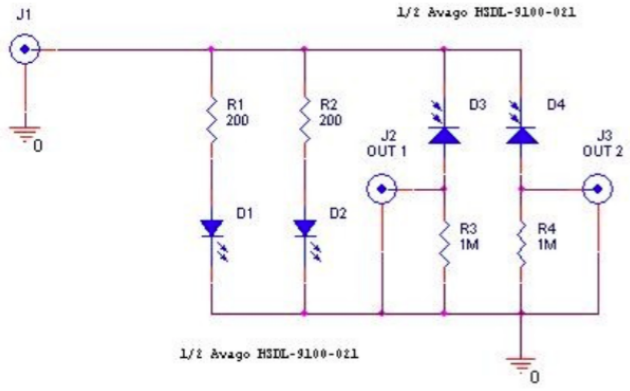

Figure 4: The readout: two pairs (emitter+receiver) of LEDs are biased to 5V via the J1 coax, and the signals extracted via the two J2 cables.

3. Data processing and parameters evaluation

In all our measurements, we manually set the pendulum in motion via the *external* rotary feedthrough and then observed the free evolution of its oscillations, as described by the well known equation for a simple harmonic oscillator:

$$\frac{d^2\theta}{dt^2} + \frac{2}{\tau}\frac{d\theta}{dt} + \frac{\kappa}{I_0}\theta = 0 \tag{1}$$

Therefore, we measured two dynamic parameters related to free oscillations of torsion pendulums: the natural frequency $f_0 = \frac{1}{2\pi}\sqrt{\frac{\kappa}{I_0}}$ (rather than resonant frequency), inverse of the free oscillation period T, and the amplitude decay time τ. A better way to compare features of pendulums with vastly different periods is to express its dissipation through the dimensionless quality factor $Q = \pi f_0 \tau$. In all instances, the pendulums had a Q factor exceeding a few thousands, i.e. high enough to make the difference between natural and resonant frequency (that is $O(Q^{-2})$ [9]) completely negligible.

From either of the two time series, one for each sensor, we can recover with some simple manipulations both the resonant frequency and the decay time of the pendulum. The recorded output of the two sensing LEDs appears as shown in fig.4.

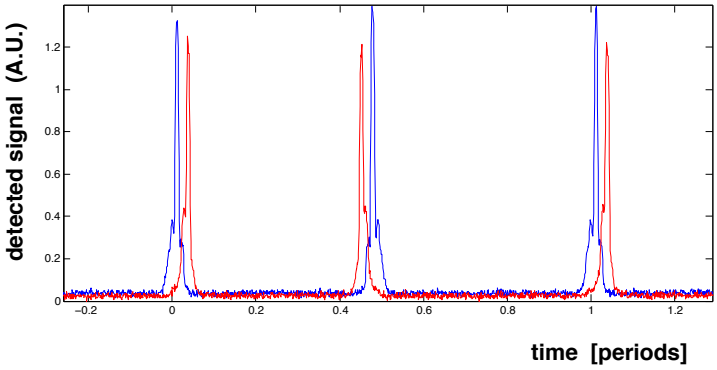

Figure 5: Each sensor (blue or red) detects the passage of the pendulum and a pulse is recorded. The order of pulse arrival depends on the sense of oscillation, but the pulse separation in time is the same

3.1. Measurement of the period of oscillation T

Determination of the resonant frequency is trivial and only requires one channel: each sensor detects two peaks every oscillation period T: these two signals are equally spaced at $T/2$ only if the detector is positioned exactly at the center of the oscillation, which is hardly ever the case. An offline analysis with a peak-finding routine provides a set of time stamps for the passing time of the pendulum hairline marker in front of the sensor. We shall separately consider the two sets of peaks that happen at times $t_k = k \cdot T/2$ with k even (or odd) integer. All peaks belonging to each set are separated in time by a whole period T: $t_{k+2} - t_k = T$; an average over the several hundreds values recorded in a typical overnight run yields a value of T with an uncertainty of 0.1% or better.
In some cases, when dissipation is relevant, it can be shown (see Appendix) that the two evaluations of the oscillation period (k odd or even) exhibit a splitting; the true value of the period T can be recovered by averaging over the two determinations. Usually, for slow decay, $\tau \gg T$, this splitting is negligible.

3.2. Q measurement with two sensors

Evaluation of the decay time constant requires both channels and a little more subtlety: To this purpose, consider a generic damped oscillation of period $T = 2\pi/\omega$ for the angular coordinate of the hairline sight of the pendulum:

$$\theta(t) = Asin(\omega t + \phi)e^{-t/\tau} \tag{2}$$

Our readout consists of two emitters + sensors separated by a small angular distance $\Delta\theta$: as seen from the oscillation axis, this is, roughly, the sensors

separation d divided by the distance from the suspending fiber: for our widest test mass: $\Delta\theta = \frac{d}{a_{max}} = 4/140 \sim 30\ mrad$.
Due to their different position, the two sensors detect the passage with a time difference Δt.
As $\Delta\theta \ll 1$ (small separation between the two sensors), this delay can be related to the pendulum velocity by

$$\Delta\theta = \dot{\theta}\Delta t. \tag{3}$$

Being the left hand side of the relation a constant, as the velocity decreases due to damping, the time delay Δt is bound to increase: this allows us to measure the damping time τ

We evaluate the time derivative of $\theta(t)$ at the times of detection $t_k = k \cdot T$ of either channel, with the additonal assumption that both sensors are close to the center of oscillation: this implies $\phi \simeq 0$:

$$\dot{\theta}(kT) = Ae^{-kT/\tau}[\omega cos(\omega kT) - \frac{1}{\tau}sin(\omega kT)] \tag{4}$$

The hypotesis of being close to the center ($sin(k\omega T) \simeq 0,\ cos(k\omega T) \simeq 1$), as well as the small damping ($\omega \gg 1/\tau$), allows us to neglect the second term with respect to the first:

$$\dot{\theta}(kT) \simeq \omega Ae^{-kT/\tau} \tag{5}$$

We now combine eq.(3) and (5), keeping in mind that $\Delta\theta$ is a constant, for any k-th detection pulse, as well as for an initial (zeroth) one:

$$\Delta\theta = Ae^{-kT/\tau}\omega\Delta t_k = A\omega\Delta t_o \tag{6}$$

A final, simple manupulation yields T/τ as the slope of a logarithmic regression:

$$\ln\left\{\frac{\Delta t_k}{\Delta t_0}\right\} = \frac{T}{\tau}k \tag{7}$$

Recalling a definition of $Q = \pi\tau/T$, it is immediate to recognize that the inverse slope of the regression is just Q/π.

We remark that the same data provide two time series (see fig. 5a) with opposite slopes, depending on wheter we consider measurements in the clockwise direction (t_k from sensor A lags that from sensor B) or conterclockwise (sensor B lags sensor A). Apart from the sign, the two time series follow the same exponential law, as shown in fig. (5b).

This method is straightforward and accurate, however, as can be seen in fig.(4), the peaks are not sharp: in some cases, even worse than shown here, this can lead to errors in the determination of the occurrence time t_k of the light peak. Indeed, the secondary peak is the result of a cross-talk from one sensor (say detector A) sensing the light emitted by the other LED (say B), due to the proximity of the mounting and the wide angle of emission. We managed to obtain better time resolution by removing (or blinding) one set and using just one LED pair, as described in the next section.

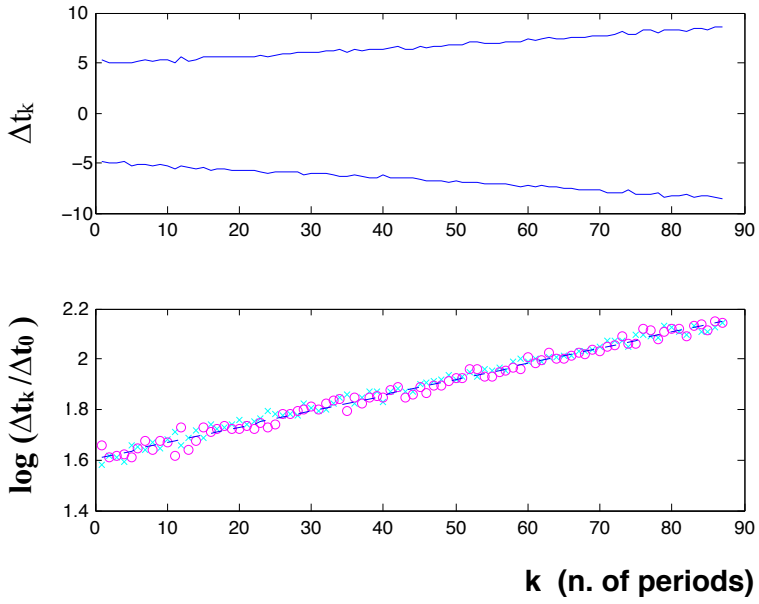

Figure 6: Plot of the time delay between signals in the two sensors $\Delta t_k = t_{k+1} - t_k$ vs the number of oscillations k. In the top pane the two series (k odd and k even) are shown. In the bottom pane, the linear regression fit on the $\ln \frac{\Delta t_k}{\Delta t_0}$ shows, as described by eq. 7, a slope of $a = 6.27 \cdot 10^{-3}$, yielding $Q = \pi/a = 500$.

3.3. Q measurement with a single sensor

Also with a single emitter-sensor pair it is possible to measure the decay time τ, using the asymmetry between the two "semiperiods" that arises if the sensor is not exactly placed at the center of oscillation, but with an angular offset s. The times of detection t_k are defined by the roots of the equation:

$$A\ sin(\omega t_k)\ e^{-t_k/\tau} = s \tag{8}$$

Fig.6 shows a graphic representation of the problem where, without loss of generality, we chose $s > 0$; we now derive an approximate solution[1] for t_k in two steps:

step 1: no damping. With the sensor centered ($s = 0$), the detection times t_k are obviously given by $\omega t_k = k\pi$; consider now the presence of a small angular offset $s \ll A$, and still no damping: we can approximate the sine near $\omega t = k\pi$

[1] A solution with a better degree of approximation is given in the Appendix, but we show here a "zeroth order" derivation that provides a correct value with an intuitive approach

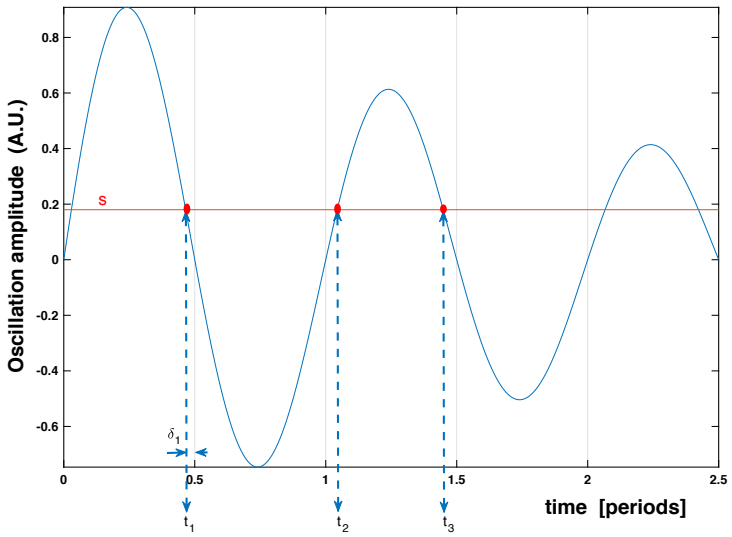

Figure 7: Threshold crossing: if peak detection is set at a threshold $s > 0$ (red line), the detection time is alternatively before (k even) or after (k odd) the time of zero crossing $kT/2$, by a small time offset $\delta = \pm(T/2\pi)(s/A)$

with its argument:

$$\omega t_k = k\pi \pm \frac{s}{A}; \qquad\qquad t_k = \; k\frac{T}{2} \pm \frac{T}{2\pi}\frac{s}{A} \tag{9}$$

It can be seen, from fig.(6) that the time of threshold crossing happens a little earlier (k even, negative sign in eq.9) or a little later (k odd, "+" sign) than the half periods $kT/2$. This offset time is indeed given by: $\delta \equiv \pm(T/2\pi)(s/A)$ and has, in absence of damping, a constant value. Consider the time intervals between two successive light peaks: they are alternatively longer and shorter than half period, by an amount 2δ; call them $T_k^{\pm} = t_{k+1} - t_k = T/2 \pm 2\delta$. In the case shown in fig.6, we have T_k^{+} for k odd, but this depends on the sign of the offset s and on the phase of the oscillation.

Define now the ratio R_k between each time interval and the entire oscillation period T:

$$R_k^{\pm} = \; \frac{T_k^{\pm}}{T} = \frac{1}{2} \pm \frac{2\delta_k}{T} = \frac{1}{2} \pm \frac{s}{\pi A} \tag{10}$$

step 2: introduce damping. We finally take into account the decay of the oscillation by substituting the constant amplitude A with $A_k = A_0\; e^{-kT/2\tau}$ into eq.(10). By taking the logarithm, we promptly derive:

$$\ln|R_k^{\pm} - \frac{1}{2}| = \ln(\frac{s}{\pi A_0}) + \frac{kT}{2\tau} \tag{11}$$

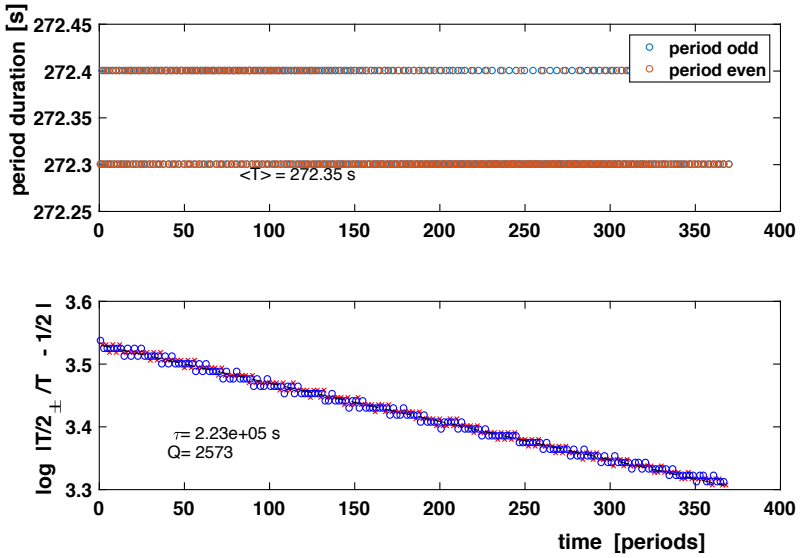

Figure 8: Evaluation of both the oscillation period and the decay time with a single sensor. The splitting of the period measurement is due to unsufficient sampling frequency. In the lower pane, the slope has been reversed, in intuitive accordance with a decay.

While both R_- and R_+ can be separately used for evaluating he decay time, the combination $|R_k^+ - R_k^-| = 2s/\pi A_k$ has proven to provide linear fits with marginally better correlation. Again, the logarithm of the quantity on the left hand side of eq.(11) grows linearly with k, with a slope $T/2\tau = \pi/2Q$. An example of this regression is shown in fig.(7)

3.4. Unwinding

Unwinding is a well known feature of metallic torsion fibers, where the equilibrium position of the pendulum (i.e. $Asin(\phi)$) slowly changes with time until a stationary situation is reached; this drift can last a few days and it usually takes place when the fiber is freshly loaded. When this happens, the center of oscillation of the pendulum drifts during the measurement, i.e. $s \to s(t)$ in eq.8. This mimicks, to the purpose of the t_k series, the effects of an additional decay. When this happens, evaluation of the period of oscillation still gives accurate results, provided that the two different determination (k odd and k even) are averaged, thus canceling the systematic offsets. However, the calculations described in previous sections to determine the Q factor no longer hold; indeed, the decay is not even exponential, exhibiting slow oscillations around a spurious decay. This behaviour is displayed in the numerical simulation of fig.8, while fig.9 shows the behaviour of a real measurement with unwinding.

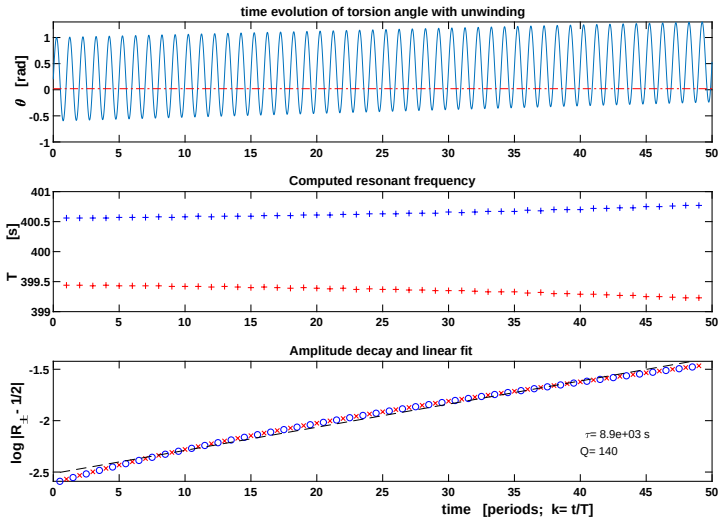

Figure 9: Numerical simulation of an oscillation in the presence of unwinding. The first pane shows the angular position $\theta(t)$ (see eq.2) with unitary amplitude A. The oscillation period (second pane), determined as described in sect. 3.1, averaging the two determinations, yields an accurate result (T=400 s). As expected, Q evaluation fails: the third pane shows an estimated Q of 140, while the input value was 4000.

4. Applications and Conclusions

We have used the apparatus and the method described above to characterize Tungsten fibers of various sizes; both the torsion constant (via the oscillation period) and the internal friction (via the decay time) were measured. Results are summarized in table 1. Due to the very low eigenfrequencies of these oscillations, a typical data taking would last overnight. Two different methods are described to measure the decay time of the pendulums: while the method with two emitter-sensor pairs is simple in the algorithm and provides redundant information, we found that the single emitter-sensor readout provides in the end more reliable results, due to the absence of secondary, ghost peaks.

We have also used this apparatus to test a new way of connecting the fiber both to the suspension point and to the inertial load, as described in section 2. As shown in table 1 the elastic constant is, as expected, unchanged; on the other hand, measurements of the the decay time did not provide conclusive evidence: we gathered data on a dozen of different pendulums, with Q measurements varying in the 1500 - 5000 range, depending on the size of the inertial member, fiber thickness, but also on the residual pressure inside the vacuum chamber that was most likely the limiting factor. The effect of air damping on the pendulums

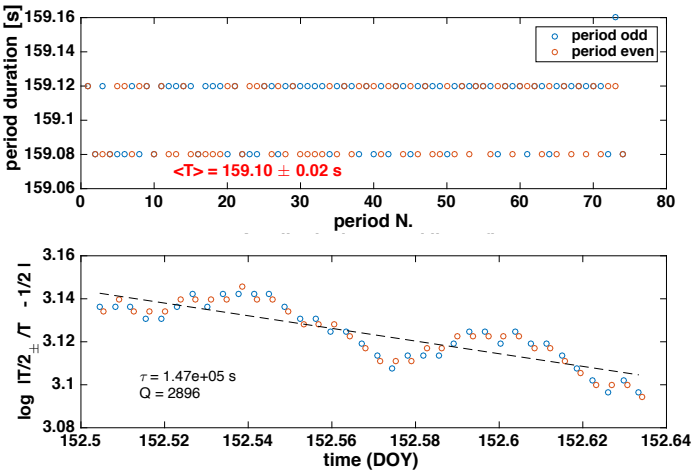

Figure 10: Actual measurement of period and Q of an oscillation in the presence of unwinding. The lower x axis is espressed in DOY (Day Of Year), as recorded for the raw data

[10] is an interesting investigation, that is however beyond the purpose of this note. Therefore, we could detect no clear effect of improvement or deterioration of the dissipation due to the new vise clamps. We have described how, with a very basic apparatus and some simple manipulations, a readout for torsion pendulums can be assembled. We believe this set-up can have applications in cases where large amplitude of oscillations must be recorded, where budget is a concern and in student labs.

Appendix - Determination of the oscillation period

We look for a better solution of eq.8; to this purpose we distinguish between the actual oscillation period T, to be determined, and its experimental evaluation T_{meas}. We expect the detection times t_k to be close to multiples of half periods:

$$\omega t_k = k\pi + \eta \qquad\qquad |\eta| \ll 1 \tag{12}$$

Substituting this into eq.8 and approximating to first order in η we obtain:

$$\pm\eta(1 - \frac{\eta}{2Q})e^{-k\pi/2Q} \simeq s/A \tag{13}$$

This second degree equation has only one root satisfying $|\eta| \ll 1$, that is: $\eta_k = \pm s/A \cdot e^{k\pi/2Q}$. With this value, eq.12 reads:

$$t_k = k\frac{T}{2} \pm \frac{Ts}{2\pi A}e^{k\pi/2Q} \tag{14}$$

Table 1: Values of torsional constant, scaled to a 1 m length, for Tungsten wire of several diameters ϕ. The values reported in second column are measured with a standard pin-clamping of the wire ends, while in the last column the measurements were taken with the news pressing vises. The data reported are compatible,within the experimental errors, with the well known scaling law. $\kappa \propto \phi^4$ (see e.g. eq. 5.2 in ref.[2])

Wire diameter ϕ (μm)	Torsion constant κ ($10^{-9} Nm/rad$)	
	pin squeeze	vise clamp
25	5.7 ± 0.1	6.0 ± 0.1
50	87.5 ± 3	89 ± 2
80	591 ± 5	585 ± 5
100	1319 ± 12	

The exponential term grows with k (i.e. with time), but remains negligible as long as $k \ll Q$. When we now evaluate the oscillation period by computing the difference between even or odd t_k's, we get:

$$T_{meas} = t_{k+2} - t_k = T \pm \frac{Ts}{2\pi A} e^{k\pi/2Q}(e^{\pi/Q} - 1) \simeq T(1 \pm \frac{s}{2AQ} e^{k\pi/2Q}) \quad (15)$$

Although the evaluation of T_{meas} gives two different (and slowly diverging) values, the true oscillation period T can be recovered by averaging the two determinations. In most cases, both $s/A \ll 1$ and $1/Q \ll 1$ and therefore the second term is uninfluential, so that $T = T_{meas}$.

Acknowledgments

This work stemmed from Mr. A. Impagnatiello's thesis, and was later supported by Istituto Nazionale di Fisica Nucleare.

Mr. Roberto Simonetti provided invaluable technical support ad advice until his untimely death. With this paper we honour his memory.

References

[1] G.T. Gillies, R.C. Ritter: *Torsion balances, torsion pendulums and related devices* Rev. Sci. Instrum. 64 (1993) 283.

[2] G. L. Baker and J. A. Blackburn: *The Pendulum: A Case Study in Physics, chapt. 5* Oxford University Press, 2005

[3] M.Bassan et al. *Torsion pendulum revisited* Phys. Lett. A377 (2013) 1555

[4] M.Bassan et al. *Approaching free fall on two degrees of freedom: simultaneous measurement of residual force and torque on a double torsion pendulum* Phys. Rev. Lett. **116**, 051104 (2016)

[5] M.Bassan et al. *Cross-talk measurement, on the double pendulum, for the LISA-Pathfinder electrostatic actuators: force to torque and torque to force cross-couplings* Astrop. Phys **97**, 19 (2018)

[6] Agilent HSDL-9100 Miniature Surface-Mount Proximity Sensor

[7] R. De Rosa et al. *An optical readout system for the drag free control of the LISA spacecraft* Astrop. Phys. **34**, 394 (2011)

[8] https://www.vermontphotonics.com/product-category/elcomat-electronic-autocollimators

[9] D S Jones *Electrical and Mechanical Oscillations, an Introduction* Routledge and Kegan (1961)

[10] C E Mungan *Frictional torque on a rotating disc* Eur. J. Phys. 33 1119 (2012)